Differences in processing of low- and high-order image statistics revealed by classification images extracted via regularized regression

Jonathan D. Victor, Ana Ashurova, and Mary M. Conte
Department of Neurology and Neuroscience
Weill Medical College of Cornell University, New York, NY 10021

INTRODUCTION

The luminance histogram and spatial correlations are two kinds of image statistics that are known to play important roles in texture segregation. In most psychophysical studies, one of these kinds of statistics is manipulated, while the other is kept constant. For example, in IID textures (Chubb et al. 1994), each check's luminance is independently chosen from a specified distribution, thus manipulating the luminance histogram while eliminating spatial correlations. In isodipole textures (Julesz et al. 1978), high-order spatial correlations are manipulated while keeping luminance and second-order statistics constant.

Maximum-entropy extension (Zhu et al., 1998) provides a means to generate textures in which luminance histograms and spatial correlations are simultaneously manipulated in a controlled fashion. We recently studied a two-parameter family of textures generated by this approach (Victor et al. 2005). We found that within this family, luminance and spatial correlation cues are processed independently (upper right portion of poster).

We then applied the method of classification images (CI's) to gain insight into the computations underlying perceptual decisions (Ahumada & Lovell, 1971). In the usual approach to extract classification images (Eckstein & Ahumada 2002), the mean stimulus associated with each perceptual decision are compared. We added two analytical ingredients. First, to identify nonlinear contributions, CI analysis was based on "derived images" (obtained by applying a local nonlinearity to each stimulus image), and not just on the original stimuli. Second, we used regularized regression to recover detail that might be overlooked by standard subtraction.

METHODS

TASK: Identify the location of the target stripe (4-AFC, top, right, bottom, left)

SUBJECTS: N=5, VA corrected to 20/20; practiced for 2 - 3 hrs

STIMULI: 11.6 deg square, viewed binocularly at 57 cm, contrast 1.0, luminance 57 cd/m², duration 200 ms, refresh: 75 Hz (Dell Trinitron Monitor)

CONDITIONS: Feedback on error in all practice and experimental blocks, 288 trials per block (8 repeats of coordinate-axis points and16 repeats of diagonal points randomized in every block, 15 such blocks/subject), 4320 trials/subject

PARAMETER SPACE

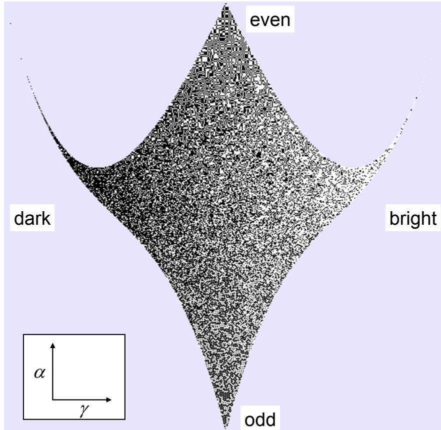

Luminance parameter: $\gamma = p\{\square\} - p\{\blacksquare\}$

$\gamma = 0$ specifies a texture with an equal number of bright and dark checks. $\gamma = 1$ specifies a texture with only bright checks. $\gamma = -1$ specifies a texture with only dark checks.

Isodipole (fourth-order correlation) parameter:

$\alpha = p\{\ldots\} - p\{\ldots\}$

$\alpha = 1$ specifies a texture in which all 2x2 blocks have an *even* number of bright checks. $\alpha = -1$ specifies a texture in which all 2x2 blocks have an *odd* number of bright checks.

STIMULI

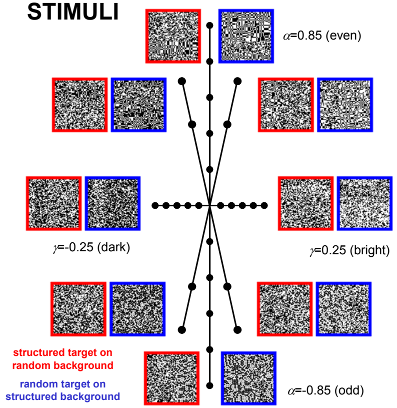

The probabilities of all 16 black-and-white configurations within 2x2 blocks are determined from α and γ via maximum entropy, along with the requirement that the block probabilities are consistent with a planar Markov process (Pickard 1980). A solution exists provided that $\gamma^4 - (1-|\gamma|)^4 \le \alpha \le \gamma^4 + (1-|\gamma|)^4$. These inequalities define the stimulus space shown above left. Maximum entropy is achieved when the probability of a particular 2x2 block that contains n bright checks is given by $[(1-\gamma)^{4-n}(1+\gamma)^n + (-1)^n(\alpha - \gamma^4)]/16$. There are no second- or third-order correlations: the probability of a pair of bright checks is $(1+\gamma)^2/4$, and the probability of a triple is $(1+\gamma)^3/8$.

The 2x2 block probabilities define a Markov propagation rule parametric in γ and α. This rule is used to generate "background" and "target" textures, with the desired values of γ and α in each region. At the border between "background" and "target", the rule is changed but the Markov chain is not re-initialized, to avoid edge artifacts.

ISO-DISCRIMINATION CONTOURS

Psychophysical performance followed a Weibull function along each direction in texture space, and a Minkowski rule adequately described how sensitivity in the oblique directions depended on sensitivity in the cardinal directions. That is, the observed fraction correct data $p_{obs}(\alpha, \gamma)$ were well-described by:

$$p_{model}(\alpha,\gamma) = 1 - \frac{3}{4}\exp\left(-\left(|\alpha/a_\alpha|^m + |\gamma/a_\gamma|^m\right)^{\frac{b}{m}}\right)$$

The Weibull sensitivity parameters a_α and a_γ were allowed to depend on the signs *of* α and γ, and on whether the target was **structured** or **random**. Note that $m=b$ corresponds to probability summation of the two cues, and that $m=2$ corresponds to elliptical iso-discrimination contours – both consistent with our data. The fits were not improved by allowing for rotation of the axes, thus indicating independent processing of these two cues.

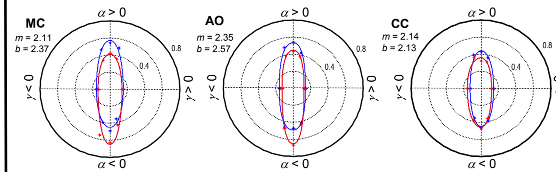

For an ideal observer, all isodiscrimination contours would be circular – a nice feature of the maximum-entropy construction.

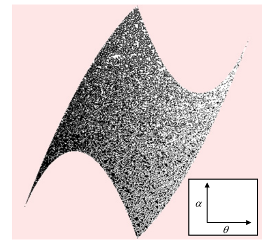

For luminance (γ) and fourth-order statistics (α), the axes of the isodiscrimination contours are parallel to the cardinal axes of texture space, indicating a lack of interaction of these statistics.

For luminance (γ) and third-order statistics (θ), isodiscrimination contours are tilted, implying an interaction.

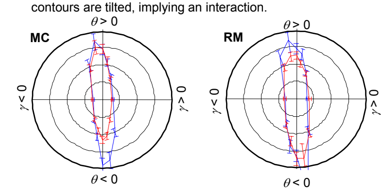

CLASSIFICATION IMAGE ANALYSIS AND RESULTS

Derived images are constructed by

- local estimation of the statistic of interest (γ: pixel luminance, or α: parity in a 2x2 block)
- optional contrast inversion, so that target is lighter than background

Derived images are then rotated so that the **perceived** target is at top, prior to analysis via subtraction or regression.

Construction of derived images

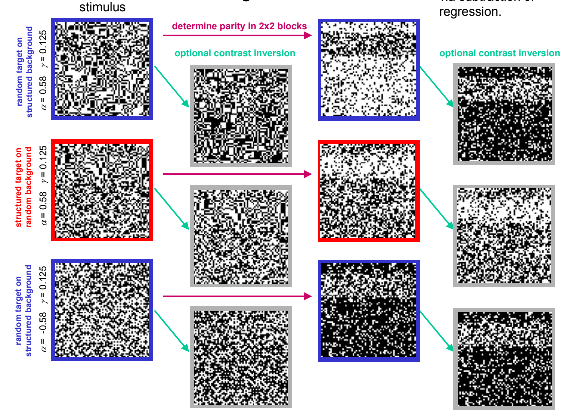

γ - derived image *α - derived image*

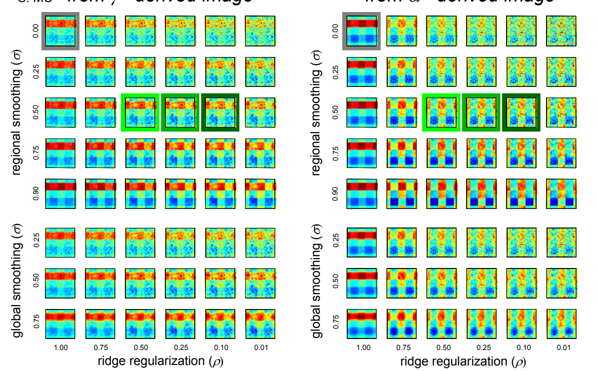

Right: classification images for each subject, calculated by subtraction (gray) and regularized regression with selected values of the ridge and smoothing parameters ρ and σ (green).

subtraction
ρ =1.00 σ =0.0

regularized regression
ρ =0.50 σ =0.5
ρ =0.25 σ =0.5
ρ =0.10 σ =0.5

Extreme right: the average value of each classification image along raster lines.

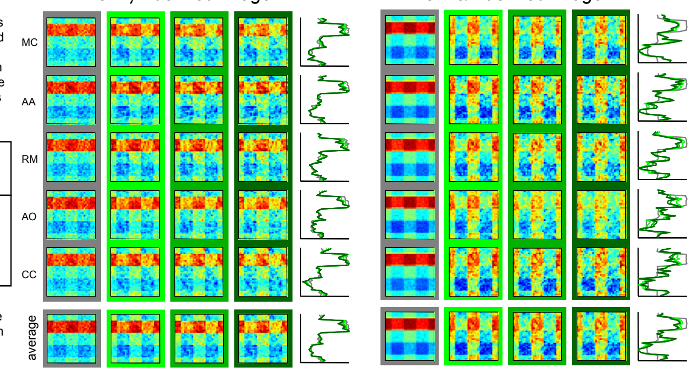

For each kind of derived image (γ and α), classification images were computed by several methods.

subtraction (reverse correlation): $CI = (\mu_{correct} - \mu_{incorrect})^T$ where $\mu_{correct}$ and $\mu_{incorrect}$ are the means of the derived images on the correct and incorrect trials.

regularized regression: $CI = M^{-1}(\mu_{correct} - \mu_{incorrect})^T$ where $M = (1-\rho)S + \rho I$, S is proportional to the covariance matrix of the derived images, and ρ is the ridge regularization parameter. $\rho = 1$ corresponds to subtraction.

penalized regression: $CI = M^{-1}(\mu_{correct} - \mu_{incorrect})^T$ where $M = (1-\sigma)[(1-\rho)S + \rho I] + \sigma P$, P is a quadratic penalty for non-smoothness, and σ controls the strength of the penalty. $\sigma = 0$ corresponds to regularized regression.

regional smoothing: P penalizes differences between adjacent pixels within target or background.

global smoothing: P penalizes differences between all adjacent pixels.

CONCLUSIONS

- The classification image method can be extended to a strongly nonlinear context via the use of "derived images".
- Regularized regression can identify details in a classification images overlooked by standard subtraction analysis.
- Statistics near a putative border play a disproportionate role in texture segregation, as might be expected from edge-enhancing mechanisms such as lateral inhibition.
- Spatial weighting of luminance statistics shows greater edge-enhancement than spatial weighting of fourth-order statistics in 3 of 5 subjects, and on average.

REFERENCES

Ahumada, A.J., Jr. and Lovell, J. (1971) Stimulus features in signal detection. Journal of the Acoustical Society of America 49, 1751-1756.

Chubb, C., Econopouly, J., and Landy, M.S. (1994) Histogram contrast analysis and the visual segregation of IID textures. J Opt Soc Am A 11, 2350-74.

Eckstein, M.P. and Ahumada, A.J., Jr. (2002) Classification images: a tool to analyze visual strategies. J Vis. 2, 1.

Hastie, T., Buja, A., and Tibshirani, R. (1995) Penalized discriminant analysis. Annals of Statistics. 23, 73-102.

Julesz, B., Gilbert, E., and Victor, J.D. (1978) Visual discrimination of textures with identical third-order statistics. Biological Cybernetics 31, 137-140.

Pickard, D.K. (1980) Unilateral Markov fields. Adv. Appl. Probab. 12, 655–671.

Victor, J.D. (2005) Analyzing receptive fields, classification images and functional images: challenges with opportunities for synergy. Nat Neurosci. 8, 1651-6

Victor, J.D., Chubb, C., and Conte, M.M. (2005) Interaction of luminance and higher-order statistics in texture discrimination. Vision Res. 45, 311-28

Victor, J.D. and Conte, M.M. (1991) Spatial organization of nonlinear interactions in form perception. Vision Res. 31, 1457-88.

Zhu, S.C., Wu, Y., and Mumford, D. (1998) Filters, random fields and maximum entropy (FRAME): Towards a unified theory for texture modeling. International Journal of Computer Vision 27, 107-126.

Supported by NIH NEI EY7977